J Therm Anal Calorim (2018) 131:2373–2380
https://doi.org/10.1007/s10973-017-6781-7

Microencapsulated myristic acid–fly ash with TiO_2 shell as a novel phase change material for building application

Murat Genc[1] · Zuhal Karagoz Genc[2]

Received: 19 June 2017 / Accepted: 24 October 2017 / Published online: 2 November 2017

Abstract The microencapsulated myristic acid with titanium dioxide (TiO_2) shell as shape-stabilized thermal energy storage materials was prepared using sol–gel method. The XRD and FT-IR techniques results presented that characteristic peaks of both myristic acid and TiO_2 can be observed in the microencapsulated myristic acid with TiO_2 shells. The phase change temperature, latent heat and thermal stability were investigated by a differential scanning calorimetry (DSC) and thermogravimetric analyzer (TGA). According to these results, the melting and freezing temperatures of the MPCM/TiO_2 shell and MPCM/TiO_2 shell–fly ash are 56.95 and 52.22 °C; 47.56 and 26.68 °C and the latent heats of melting and freezing are 96.64 kJ kg^{-1}; 97.72 and 23.43 kJ kg^{-1}; and 22.57 kJ kg^{-1}, respectively. TGA results certified that the addition of fly ash improved thermal stability. In particular, MPCM/TiO_2 shell displays good thermal reliability after 1000 repeated melting/freezing cycling.

Keywords Phase change material · Microencapsulating · Myristic acid · Thermal properties

✉ Zuhal Karagoz Genc
zuhalkaragoz23@gmail.com

[1] Department of Chemistry, Faculty of Science and Arts, Adiyaman University, 02040 Adiyaman, Turkey

[2] Department of Metallurgy and Materials Engineering, Engineering Faculty, Adiyaman University, 02040 Adiyaman, Turkey

Introduction

In recent years, the shortages of fossil fuels and increasing energy depletion have been a big trouble for the development of the human society. Thus, efficient ways of energy storage and recovery as well as the investigation of new energy resources have attracted much attention [1–3]. Phase change materials have an important role for various applications in air-conditioning systems [4–7], building energy conversation [8–10] and the solar heating systems [11–13]. The various available PCMs melt and solidify at a broad range of temperatures, which are categorized into two main groups; organic (paraffin, fatty acids/esters etc.) and inorganic (salt hydrates) materials. When organic PCMs compared with inorganic PCMs, organic PCMs melt and freeze repeatedly without degradation of their latent heat of fusion and phase segregation. Organic PCMs have high latent heat storage capacity, low vapor pressure, self-nucleating behavior, good thermal and chemical stability [14–16]. However, they need encapsulating to avoid leakage [17, 18], of the melted PCMs and high volume changes [19] during the phase change process. This process can be performed by encapsulating of the PCM in a polymeric structure, such as styrene–butadiene–styrene (SBS), copolymer [20] and high-density polyethylene (HDPE) [21–23], melamine–formaldehyde (MF) resin [24] and urea–formaldehyde (UF) resin [25]. While using polymeric shell in particular application, polymer might be inclined to degrade and release noxious gas continuously that leads to health and environmental problems. In addition of these, some applications of polymeric shells are limited because of their poor thermal stability low heat conductivity and mechanical strength [26], flammability [27]. So, using the inorganic shells has been achieved great interest recently [28]. The reactivity of the PCM within the outside

environment can be decreased by encapsulating with an inorganic shell [29]. The TiO_2 shell materials have high surface area and tunable pore size with good thermal stability, lower the flammability and no leakage during melting of PCMs. In situ polymerization [30], spray drying, complex conservation [31], interfacial polymerization [29], miniemulsion polymerization [32] and sol–gel method are encapsulating methods for PCMs. But, the fluid's viscosity of the large particle sizes of the microencapsulated PCMs is not appropriate for repeated cycling in functionally thermal fluids fields. So, PCM nanocapsules must be prepared with smaller particle sizes as compared with microcapsules [29].

This study, therefore, has focused on synthesizing nanocapsules of palmitic acid with silica shell via the sol–gel method and studying the thermal characterization. Myristic acid is favorable organic PCM for thermal energy storage, melting at 62.50 °C with a latent heat of 178.7 kJ kg^{-1}, and solidifying at 42.32 °C with a latent heat of 177.5 kJ kg^{-1} [33, 34]. Fly ash is used for investigation of building application of myristic acid/TiO_2. Fly ash, a byproduct of coal combustion, can be recycled. While fly ash's safety is up for debate, it is considered a sustainable material when reused in bricks or other building materials. As far as the authors are aware, there is no investigation reported in the literature on the chemical and morphological characterization, particle size distribution, thermal stability and long-term reliability of the myristic acid-fly ash/TiO_2 for the potential application in buildings.

Experimental

Materials

All chemical were analytical grade and used without further purification. Myristic acid, tetra-*n*-butyl titanate (TNBT) and sodium dodecyl sulfate (SDS) were purchased from Alfa Aesar. Fly ash was provided from Technology Faculty in Firat University.

The preparation of MPCM/TiO_2 shell

Myristic acid (10 g) and SDS (1.75 g) were added into deionized water to obtain an oil/water (o/w) emulsion in a beaker. The emulsion is kept at 60 °C for 60 min under constant magnetic stirring. After the completion of emulsification process, 12.5 TNBT and 50 mL absolute EtOH solution was added drop-wise under magnetic stirring. The solution was kept at 60 °C for 12 h to complete the hydrolysis and condensation of TNBT. The resultant microcapsules were washed and dried in a vacuum over at 40 °C for 24 h.

The preparation of MPCM/TiO_2 shell–fly ash

The myristic acid/fly ash composite sample used in this work was manufactured by the direct impregnation method. During the preparation of composites, firstly phase change material and fly ash were heated at 60 °C until the myristic acid was completely melted and mixed with hand. In the next step, stirring was continued with a mechanical stirrer approximately 2 h. At the end of process, the sol–gel mixture was obtained according to the preparation of MPCM/TiO_2 shell procedure.

Characterization of MPCM/TiO_2 shell and MPCM/TiO_2 shell–fly ash

The structural analysis of MPCM/TiO_2 shell and MPCM/TiO_2 shell–fly ash was analyzed by using FT-IR spectrometer. The spectra were recorded on a Perkin-Elmer infrared spectrometer as ATR-IR with a resolution of 4 cm^{-1} in the range of 650–4000 cm^{-1}. The morphology and microstructure of the MPCM/TiO_2 shell and MPCM/TiO_2 shell–fly ash were observed using a scanning electronic microscope (SEM, LEO 440 model). The thermal properties of PCMs were obtained using a differential scanning calorimeter (DSC, Shimadzu 60 WS), and DSC curve is tested with a heating rate of 10 °C/min in nitrogen atmosphere. The thermal stability of MPCM/TiO_2 shell and MPCM/TiO_2 shell–fly ash was studied by means of thermogravimetry on a Shimadzu TA-60WS from room temperature to 600 °C with a heating rate of 10 °C min^{-1} in air atmosphere. The XRD measurements were taken in a Rigaku RadB-DMAX II diffractometer using Cu–Ka ($k = 1.5405$ Å) radiation. The thermal reliability of the MPCM/TiO_2 shell and MPCM/TiO_2 shell–fly ash was evaluated with respect to change in the phase temperatures and latent heats after large number of thermal cycling. The thermal cycling was done by Applied Biosystem 96-well Thermal Cycler.

Results and discussion

FT-IR analysis of MPCM/TiO_2 shell and MPCM/TiO_2 shell–fly ash

The FT-IR spectra of myristic acid, MPCM/TiO_2 shell and MPCM/TiO_2 shell–fly ash are shown in Fig. 1. Characteristic vibration bands of myristic acid, TiO_2 and fly ash can be clearly seen in the curve of MPCM/TiO_2 shell and MPCM/TiO_2 shell–fly ash. In the spectrum of the myristic acid, the peaks at 2958–2851 cm^{-1} can be assigned to the stretching vibrations of aliphatic – CH groups. Beside these peaks, 1469–1198 cm^{-1} is ascribed to the bending vibrations of – CH_2, – CH and C–C groups, respectively

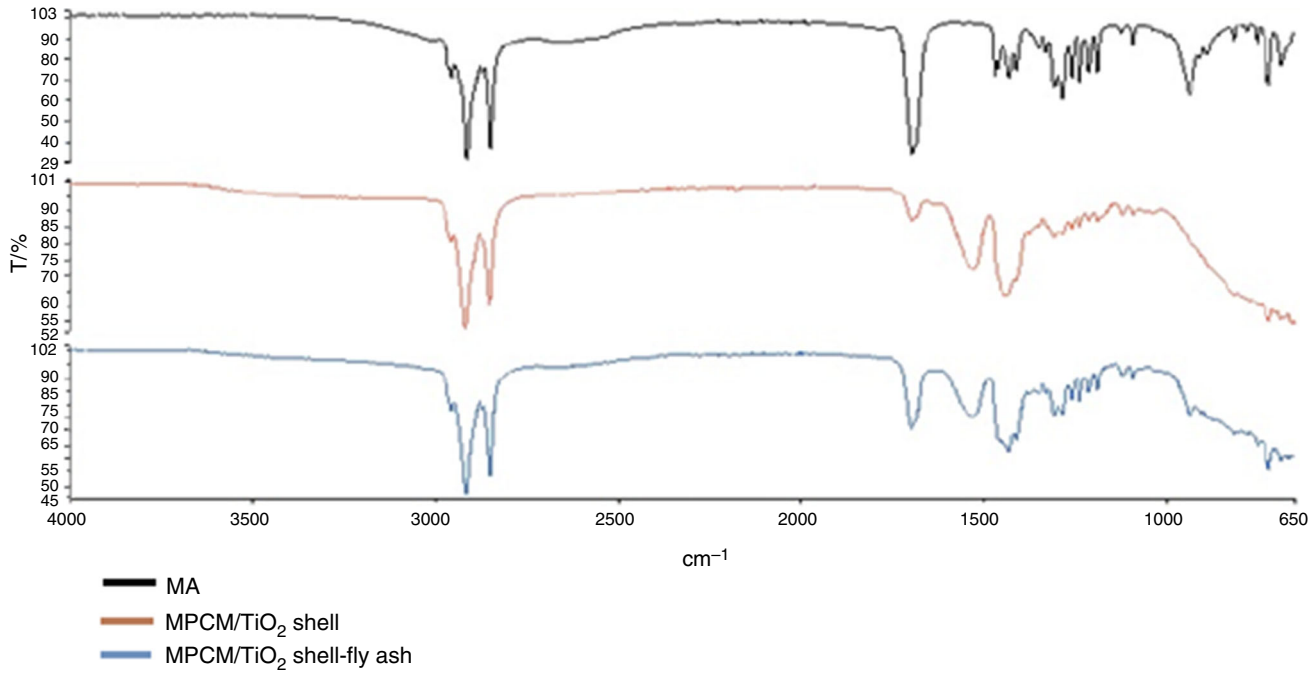

Fig. 1 FT-IR spectrum of myristic acid (MA), MPCM–TiO_2 shell and MPCM/TiO_2 shell–fly ash

[35]. The peaks at 1685 cm^{-1} can be ascribed to the stretching vibration of the C=O group in myristic acid. The peak at 1654 cm^{-1} is the characteristic absorption peak for the stretching vibration of C=C group [36]. The peak at 1533 cm^{-1} is the characteristic absorption peak for TiO_2. According to these data, there is no chemical reaction between myristic acid, TiO_2 shell and fly ash.

XRD patterns of the microencapsulated myristic acid with TiO_2 shell and MPCM/TiO_2 shell–fly ash

Figure 2 illustrates the XRD patterns of myristic acid, TiO_2, MPCM–TiO_2 shell and MPCM/TiO_2 shell–fly ash. The XRD pattern of myristic acid is present in Fig. 2a. The two sharp peaks at 8° and 14° are attributed to the crystallization of the myristic acid [37]. In Fig. 2b, there is a flat peak at around 24° that indicates that TiO_2 shell has an amorphous structure. As seen in Fig. 2c, d, the XRD patterns of the MPCM/TiO_2 shell and MPCM/TiO_2 shell–fly ash include both the peaks of the myristic acid and the flat peak of the TiO_2. This result illustrates that crystal structure of the myristic acid remains unchanged during the synthesis process.

Microstructure and morphology of the microencapsulated myristic acid with TiO_2 shell and MPCM/TiO_2 shell–fly ash

Figure 3 shows the SEM photograph of MPCM–TiO_2 shell and MPCM/TiO_2 shell–fly ash. As shown in Fig. 3, the

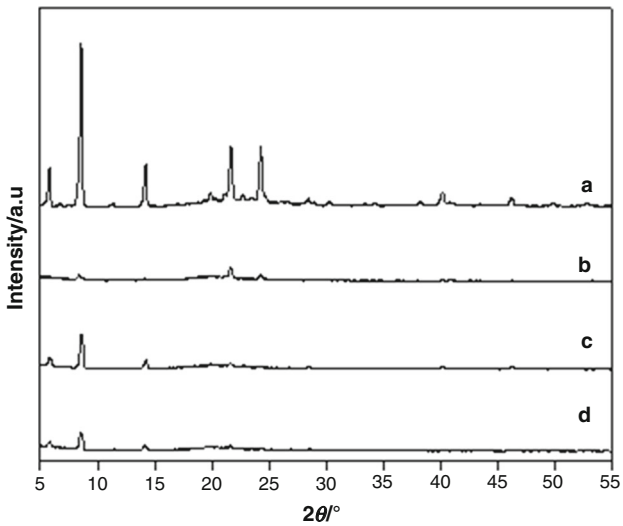

Fig. 2 XRD spectra of *a* myristic acid, *b* TiO_2, *c* MPCM–TiO_2 shell and *d* MPCM/TiO_2 shell–fly ash

myristic acid is well encapsulated in the TiO_2 shell and the TiO_2 shell avoids the myristic acid from leaking although the myristic acid was melted by the electric beam when SEM analyses were taken. The SEM photographs of all two samples illustrate the spherical structure of nanocapsules and also their smooth surfaces. Comparing Fig. 3b, c, it could be seen that the surfaces of the MPCM/TiO_2 shell–fly ash are more rippled than that of the MPCM/TiO_2 shell. The reason could be explained as follows: contraction coefficient of fly ash and the lower density of the TiO_2

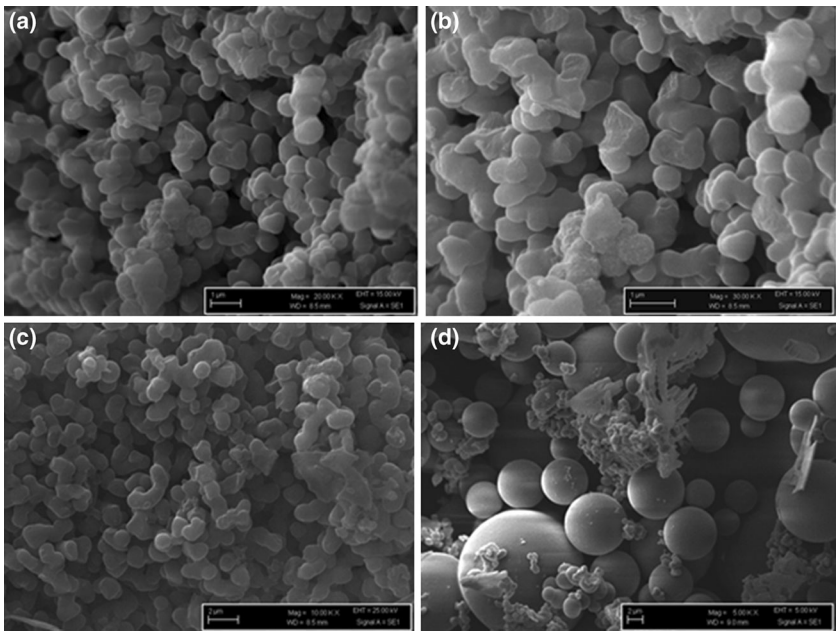

Fig. 3 SEM images of **a**, **b** MPCM/TiO_2 shell, **c**, **d** MPCM/TiO_2 shell–fly ash

compared with the MPCM/TiO_2 may lead to the shrinkage of the shells when the microcapsules cooled down, and thus ripples appeared. Beside these, the excessive TiO_2 oligomers agglomerate on the surface of the microcapsules.

Thermal properties of the MPCM/TiO_2 shell and MPCM/TiO_2 shell–fly ash

The thermal properties of the MPCM/TiO_2 shell and MPCM/TiO_2 shell–fly ash were determined by using differential scanning calorimetry. The DSC curves, the phase change temperatures and enthalpies of the PCMs are illustrated in Figs. 3–5 and Table 1. The melting and solidifying temperatures of the myristic acid are 62.50 and 42.32 °C, respectively. The peak temperature values of MPCM–TiO_2 shell and MPCM/TiO_2 shell–fly ash were determined as 56.95 and 52.22 °C for melting phase change; 47.56 and 26.68 °C for freezing phase change. As shown in Table 1, MPCM–TiO_2 shell has higher latent heat value than MPCM/TiO_2 shell–fly ash in the melting and solidifying processes.

According to the DSC results, phase change temperatures of the MPCM/TiO_2 shell–fly ash are slightly lower for freezing. This is the result from the high thermal conductivity of the matrix material. As seen in Table 1, the melting and solidifying latent heats of the composites drop with the decrease in the myristic acid content because in thermal energy storage systems, myristic acid plays an important role in operating systems.

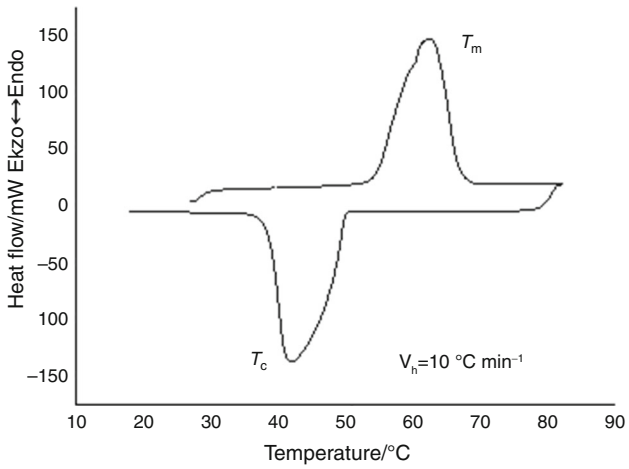

Fig. 4 DSC spectrum ofthe myristic acid

For these reasons, the thermal properties of PCMs must be determined by using the encapsulating ratio and encapsulation efficiency. They can be defined according to equations shown below [38–41]

$$\omega = \frac{\Delta H_{\mathrm{m,MPCMs}} + \Delta H_{\mathrm{c,MPCMs}}}{\Delta H_{\mathrm{m,myristicacid}} + \Delta H_{\mathrm{c,myristic\ acid}}}$$

where $\Delta H_{\mathrm{m,MPCM-TiO_2}}$ and $\Delta H_{\mathrm{s,MPCM-TiO_2}}$ are the latent heat of melting and crystallization of the microencapsulated MPCM/TiO_2 shell, $\Delta H_{\mathrm{m,myristic\ acid}}$ and $\Delta H_{\mathrm{c,myristic\ acid}}$ latent heat of melting and solidification of the pure myristic acid, respectively, for the encapsulating

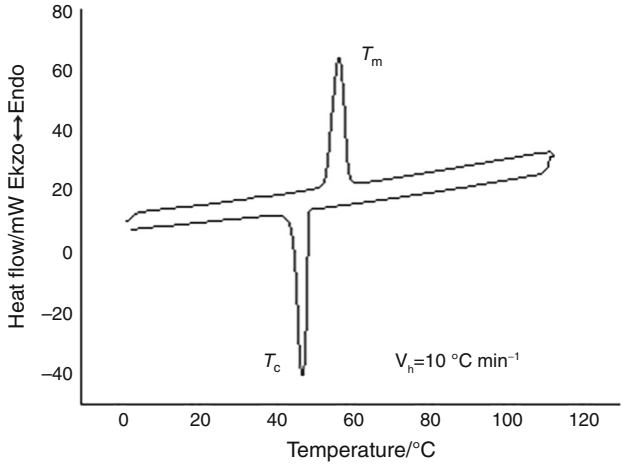

Fig. 5 DSC spectrum of the MPCM/TiO_2 shell

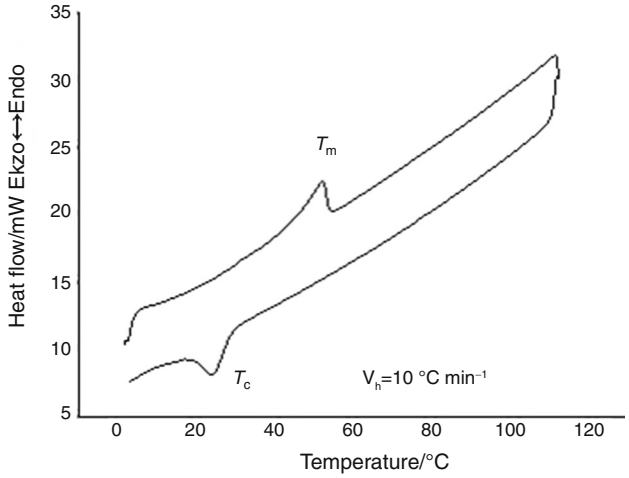

Fig. 6 DSC spectrum of the MPCM/TiO_2 shell–fly ash

ratio calculations of the MPCM/TiO_2 shell–fly ash. The encapsulating ratio indicates the effective performance of the PCMs inside the capsules, so by increasing the encapsulation ratio, leaks proof characteristic of microcapsules decrease and the mechanical strength. The melting and crystallizing enthalpies of the MPCM/TiO_2 shell and MPCM/TiO_2 shell–fly ash were found to be 96.64 and 97.72 kJ kg^{-1}, respectively, which was slightly lower than the expected values according to the myristic acid content (54.11%). The difference might be explained by thermal isolation effect of the titanium shell. It is notable in Table 1 that the encapsulating values of MPCM/TiO_2 shell–fly ash are much lower than MPCM/TiO_2 shell indicating that not all of titania precursors (TBT) have converted into TiO_2 shell in the sol–gel process. Actually, some of TBT were directly precipitated as solid particle rather than assembled on the surfaces of myristic acid-fly ash droplets through the synthesis process, resulting in the lower encapsulating efficiency of myristic acid. According to these results, the latent heats of melting and freezing of MPCM/TiO_2 shell–fly ash are 23.43 and 22.57 kJ kg^{-1}, respectively.

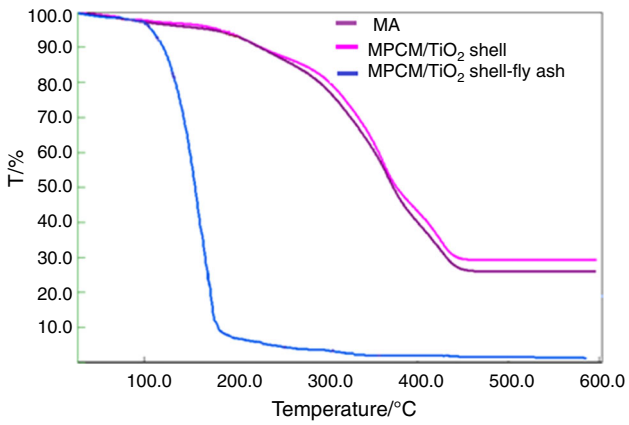

Fig. 7 TGA spectrum of the Myristic acid, MPCM–TiO_2 shell, MPCM/TiO_2 shell fly ash

Thermal stability of the myristic acid, MPCM/TiO_2 shell and MPCM/TiO_2 shell–fly ash

TGA was used to determine thermal stability of the prepared composite PCMs. Figure 7 illustrates the mass loss curves of myristic acid, MPCM/TiO_2 shell and MPCM/TiO_2 shell–fly ash. There is a single degradation process 75.4–270 °C for myristic acid because of the decomposition of fatty acid. MPCM/TiO_2 shell and MPCM/TiO_2

Table 1 The changes in thermal properties of the MPCM/TiO_2 shell and MPCM/TiO_2 shell–fly ash

Sample name	MPCM/TiO_2 shell mass%	Melting		Crystallization	
		Melting temperature T_m/°C	Melting latent heat ΔH_m/kJ kg^{-1}	Freezing temperature T_c/°C	Freezing latent heat ΔH_c/kJ kg^{-1}
Pure myristic acid	100	62.50	178.7	42.32	177.5
MPCM/TiO_2 shell	54.11	56.95	96.64	47.56	97.72
MPCM/TiO_2 shell–fly ash	13.01	52.22	23.43	26.68	22.57

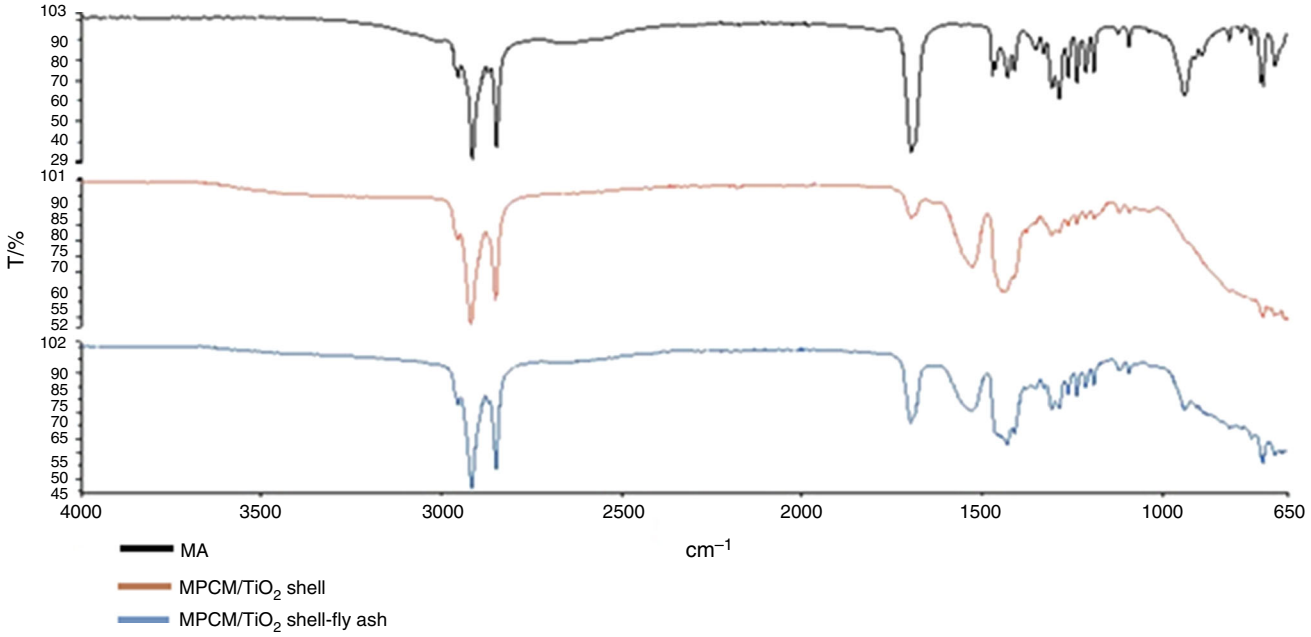

Fig. 8 FT-IR spectrum of myristic acid (MA), MPCM/TiO_2 shell and MPCM/TiO_2 shell–fly ash after 1000 thermal cycling

shell–fly ash rarely in the temperature range, in the temperature range, and the initial decomposition temperatures around 240 and 260 °C. Furthermore, no decomposition is observed for both MPCM/TiO_2 shell and MPCM/TiO_2 shell–fly within 100 °C, showing high thermal stability in low-temperature applications. Moreover, the mass loss ratio of the MPCM/TiO_2 shell and MPCM/TiO_2 are about 76.6 and 72.8%, respectively.

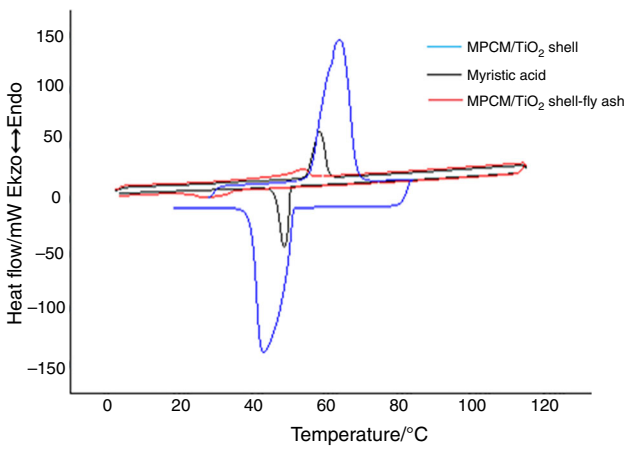

Fig. 9 DSC spectrum of the MPCM/TiO_2 shell, myristic acid and MPCM/TiO_2 shell-fly ash after 1000 thermal cycling

Thermal reliability of the MPCM/TiO_2 shell and MPCM/TiO_2 shell–fly ash

Leakage must be avoided during the phase change, if one would like to use PCM-containing microcapsules for heat storage. To analyze the potential leakage, the microcapsules were 1000 times heated and subsequently cooled. The heat storage and chemical decompositions of the MPCM/TiO_2 shell and MPCM/TiO_2 shell–fly ash were investigated by DSC and FT-IR after thermal cycles. As seen in Fig. 8, the frequency values of the characteristic peaks unchanged after 1000 thermal cycling. These results show that the chemical structures of the PCMs were not affected by thermal cycling. It was presumed that if the heat capacity of microcapsules did not change after thermal cycling test, the PCM did not leakage from the composites.

In the event of leakage, significant decrease in heat capacity could be observed. In contrast, the melting and crystallizing enthalpies of MPCM/TiO_2 shell (Fig. 9) decreased only slightly after 1000 heating–cooling cycles,

Table 2 The changes in thermal properties of the MPCM/TiO_2 shell and MPCM/TiO_2 shell–fly ash after 1000 thermal cycler

Sample name	Melting		Crystallization	
	Melting temperature T_m/°C)	Melting latent heat ΔH_m/kJ kg^{-1}	Freezing temperature T_m/°C	Freezing latent heat ΔH_c/kJ kg^{-1}
MPCM/TiO_2 shell	55.88	79.09	52,47	16.08
MPCM/TiO_2 shell–fly ash	41.74	76.37	24,85	13.09

although the heat storage capacity reduction of MPCM/TiO_2 shell–fly ash was not negligible. This result confirms that the myristic acid-fly ash adsorption is weak than that of the myristic acid, and the leakage of latter MPCM/TiO_2 shell–fly ash may be higher than acceptable for real use (Table 2).

Conclusions

In this work, shape-stabilized microencapsulated phase change materials were prepared by using sol–gel method. In the microcapsules, the myristic acid acted as phase change material for thermal energy storage, TiO_2 was used as shell material to prevent the myristic acid from leakage and improve the thermal stability of the microcapsules, and fly ash was added to determine of using as a building material. The myristic acid was well microencapsulated with TiO_2 shell, and there was no chemical interaction between the myristic acid, TiO_2 and fly ash and the crystal structure of them remained unchanged. In accordance with FT-IR, SEM and XRD results, the myristic acid is well encapsulated, melts at 56.95 °C with a latent heat of 96.64 kJ kg^{-1} and solidifies 47.56 °C with a latent heat of 97.72 kJ kg^{-1}. Beside these, MPCM/TiO_2 shell–fly ash melts at 52.22 °C with a latent heat of 23.43 kJ kg^{-1} and solidifies 26.68 °C with a latent heat of 22.57 kJ kg^{-1}. The well formed TiO_2 shell has good thermal reliability and can prevent the leakage of the microencapsulated MPCM/TiO_2 shell while MPCM/TiO_2 shell–fly ash is not revealed good thermal reliability. Based on all results, MPCM/TiO_2 shell could be used as shape-stabilized PCMs for thermal energy storage.

References

1. Baetens R, Jelle BP, Gustavsen A. Phase change materials for building applications: a state-of-the-art review. Energy Build. 2010;42:1361–8.
2. Cheng WL, Zhang RM, Xie K, Liu N, Wang J. Heat conduction enhanced shape-stabilized paraffin/HDPE composite PCMs by graphite addition: preparation and thermal properties. Sol Energy Mater Sol Cells. 2010;94:1636–42.
3. Sari A, Karaipekli A. Preparation, thermal properties and thermal reliability of palmitic acid/expanded graphite composite as form-stable PCM for thermal energy storage. Sol Energy Mater Sol Cells. 2009;93:571–6.
4. Sharma A, Shukla A, Chen CR, Dwivedi S. Development of phase change materials for building applications. Energy Build. 2013;64:403–7.
5. Lam PL, Yuen MCW, Kan CW, Wong RSM, Cheng GYM, Lam KH, Gam-bari R, Kok SHL, Chui CH. Development of calendula oil/chitosan microcapsules and their biological safety evaluation. Aust J Chem. 2012;65:72–80.
6. Lin P, Tao QH, Zhang SD, Wang SS, Zhang J, Wang SH, Wang ZY, Zhang ZP. Preparation, characterization and thermal properties of micro-encapsulated phase change materials. Sol Energy Mater Sol Cells. 2012;98:66–70.
7. Schossig P, Henning HH, Gschwander S, Haussmann T. Microencapsulated phase change materials integrated into construction materials. Sol Energy Mater Sol Cells. 2005;89:297–306.
8. Wyss A, Cordente N, Von Stockar U, Marison IW. A novel approach for the extraction of herbicides and pesticides from water using liquid-core microcapsules. Biotechnol Bioeng. 2004;87:734–42.
9. Song SK, Dong LJ, Chen S, Xie HA, Xiong CX. Stearic–capric acid eutectic/activated-attapulgiate composite as form-stable phase change material for thermal energy storage. Energy Convers Manag. 2014;81:306–11.
10. Li HR, Jiang M, Dong LJ, Xie HA, Xiong CX. Aqueous preparation of polyethylene glycol/sulfonated graphene phase change composite with enhanced thermal performance. Energy Convers Manag. 2013;75:482–7.
11. Zou Y, Tuo HF, Hrnjak PS. Modeling refrigerant maldistribution in microchannel heat exchangers with vertical headers based on experimentally developed distribution results. Appl Therm Eng. 2014;64:172–81.
12. Cao L, Tang F, Fang G. Synthesis and characterization of microencapsulated paraffin with titanium dioxide shell as shape-stabilized thermal energy storage materials in buildings. Energy Build. 2014;72:31–7.
13. Fang G, Li H, Chen Z, Liu X. Preparation and characterization of flame retardant *n*-hexadecane/silicon dioxide composites as thermal energy storage materials. J Hazard Mater. 2010;181:1004–9.
14. Yang H, Feng L, Wang C, Zhao W, Li X. Confinement effect of SiO_2 framework on phase change of PEG in shape-stabilized PEG/SiO_2 composites. Eur Polym J. 2012;48:803–10.
15. Zhang S, Wang S, Zhang J, Jiang Y, Ji Q, Zhang Z, Wang Z. Increasing phase change latent heat of stearic acid via nanocapsule interface confinement. J Phys Chem C. 2013;117:23412–7.
16. Tan HB, Li YZ, Tuo HF. Experimental study on liquid/solid phase change for cold energy storage of liquefied natural gas (LNG) refrigerated vehicle. Energy. 2010;35:1927–35.
17. Silva LS, Rodriguez JF, Romero A, Borreguero AM, Carmona M, Sanchez P. Microencapsulation of PCMs with a styrene-methly methacrylate copolymer shell by suspension-like polymerization. Chem Eng J. 2010;157:216–22.
18. Teng TP, Cheng CM, Cheng CP. Performance assessment of heat storage by phase change materials containing MWCNTs and graphite. Appl Therm Eng. 2013;50:637–44.
19. Cho JS, Kwon A, Cho CG. Microencapsulation of octadecane as a phase-change material by interfacial polymerization in an emulsion system. Colloid Polym Sci. 2002;280:260–6.
20. Zhang XX, Fan YF, Tao XM, Yick KL. Fabrication and properties of microcapsules and nanocapsules containing *n*-octadecane. Mater Chem Phys. 2004;88:300–7.
21. Fang GY, Li H, Yang F, Liu X, Wu SM. Preparation and characterization of nano-encapsulated *n*-tetradecane as phase change material for thermal energy storage. Chem Eng J. 2009;153:217–21.
22. Chio JK, Lee JG, Kim JH, Yang HS. Preparation of microcapsules containing phase change materials as heat transfer media by in situ polymerization. J Ind Eng Chem. 2001;7:358–62.
23. Salunkhe PB, Shembekar PS. A review on effect of phase change material encapsulation on the thermal performance of a system. Renew Sustain Energy. 2012;16:5603–16.

24. Zhang T, Wang Y, Shi H, Yang WT. Fabrication and performances of new king microencapsulated phase change material based on stearic acid core and polycarbonate shell. Energy Convers Manag. 2012;64:1–7.
25. Kenisarin M, Mahkamov K. Solar energy storage using phase change materials. Renew Sustain Energy Rev. 2007;11:1913–65.
26. Cho K, Choi SH. Thermal characteristics of paraffin in a spherical capsule during freezing and melting processes. Int J Heat Mass Transf. 2000;43:3183–96.
27. Wang X, Zhang YP, Xiao W, Zeng RL, Zhang QL, Di HF. Review on thermal performance of phase change energy storage building envelope. Chin Sci Bull. 2009;54:920–8.
28. Li H, Liu X, Fang G. Preparation and characteristics of *n*-nonadecane/cement composites as thermal energy storage materials in buildings. Energy Build. 2010;42:1661–5.
29. Li B, Liu T, Hu L, Wang Y, Gao L. Fabrication and properties of microencapsulated paraffin@SiO_2 phase change composite for thermal energy storage. ACS Sustain Chem Eng. 2013;1:374–80.
30. Zhou D, Zhao CY, Tian Y. Review on thermal energy storage with phase change materials (PCMs) in building applications. Appl Energy. 2012;92:593–605.
31. Wang WL, Yang XX, Fang YT, Ding J, Yan JY. Enhanced thermal conductivity and thermal performance of form-stable composite phase change materials by using beta-Aluminum nitride. Appl Energy. 2009;86:1196–200.
32. Sun YJ, Wang SW, Xiao F, Gao D. Peak load shifting control using different cold thermal energy storage facilities in commercial buildings: a review. Energy Convers Manag. 2013;71:101–14.
33. Sharma RK, Ganesan P, Tyagi VV. Long term thermal and chemical reliability study of different organic phase change materials for thermal energy storage applications. J Therm Anal Calorim. 2016;124(3):1357–66.
34. Tang B, Wang Y, Qiu M, Zhang S. A full-band sunlight-driven carbon nanotube/PEG/SiO_2 composites for solar energy storage. Sol Energy Mater Sol Cells. 2014;123:7–12.
35. Ince S, Seki Y, Ezan MA, Turgut A, Erek A. Thermal properties of myristic acid/graphite nanoplates composite phase change materials. Renew Energy. 2015;75:243–8.
36. Hawes DW, Feldman D. Absorption of phase change materials in concrete. Sol Energy Mater Sol Cells. 1992;18(6):201–16.
37. Zeng J-L, Zhu F-R, Yu S-B, Xiao Z-L, Yan W-P, Zheng S-H, Zhang L, Sun LX, Cao Z. Myristic acid/polyaniline composites as form stable phase change materials for thermal energy storage. Sol Energy Mater Sol Cells. 2013;114:136–40.
38. Yu SY, Wang XD, Wu DZ. Microencapsulation of *n*-octadecane phase change material with calcium carbonate shell for enhancement of thermal conductivity and serving durability: synthesis, microstructure, and performance evaluation. Appl Energy. 2014;114:632–43.
39. Zhang HZ, Wang XD. Synthesis and properties of microencapsulated *n*-octadecane with polyurea shells containing different soft segments for heat energy storage and thermal regulation. Sol Energy Mater Sol Cells. 2009;93:1366–76.
40. Fang Y, Liu X, Liang X, Liu H, Gao X, Zhang Z. Ultrasonic synthesis and characterization of polystyrene/*n*-dotriacontane composite nanoencapsulated phase change material for thermal energy storage. Appl Energy. 2014;132:551–6.
41. Jiang F, Wang X, Zhang YP. A new method to estimate optimal phase change material characteristic in a passive solar room. Energy Convers Manag. 2011;52:2437–41.